

Gene expression profile of zebrafish exposed to hypoxia during development

Christopher Ton,^{1,2} Dimitri Stamatou,² and Choong-Chin Liew^{1,2}

¹Department of Laboratory Medicine and Pathobiology, University of Toronto, Toronto, Ontario, M5G 1L5, Canada; and ²Cardiovascular Genome Unit, Brigham and Women's Hospital, Harvard Medical School, Boston, Massachusetts 02115

Submitted 27 September 2002; accepted in final form 13 January 2003

Ton, Christopher, Dimitri Stamatou, and Choong-Chin Liew. Gene expression profile of zebrafish exposed to hypoxia during development. *Physiol Genomics* 13: 97–106, 2003. First published January 14, 2003; 10.1152/physiolgenomics.00128.2002.—Understanding how vertebrates respond to hypoxia can have important clinical implications. Fish have evolved the ability to survive long exposure to low oxygen levels. However, little is known about the specific changes in gene expression that result from hypoxia. In this study we used a zebrafish cDNA microarray to examine the expression of >4,500 genes in zebrafish embryos exposed to 24 h of hypoxia during development. We tested the hypotheses that hypoxia changes gene expression profile of the zebrafish embryos and that these changes can be reverted by reexposure to a normoxic (20.8% O₂) environment. Our data were consistent with both of these hypotheses: indicating that zebrafish embryos undergo adaptive changes in gene expression in response to hypoxia. Our study provides a striking genetic portrait of the zebrafish embryos' adaptive responses to hypoxic stress and demonstrates the utility of the microarray technology as a tool for analyzing complex developmental processes in the zebrafish.

Danio rerio; cDNA microarray

HYPOXIA IS IMPORTANT in both biomedical and environmental contexts and requires rapid adaptive changes in metabolic organization. Fish live and survive in environments with low and variable levels of oxygen. Unlike mammals, which have a limited capacity to withstand long exposure to hypoxia, fish have evolved various biochemical, physiological, and behavioral adaptations that enable them to survive with little oxygen. Several studies have investigated the adaptive response of fish to low oxygen levels. For example, it has been shown that in the hypoxia-tolerant goby fish, *Gillichthys mirabilis*, prolonged exposure to hypoxia (6 days) led to changes in gene expression (15). Under hypoxic conditions, *G. mirabilis* showed a variety of responses to hypoxia, including a shutting down of major energy-requiring processes such as protein synthesis, locomotion, and suppression of cell growth and

proliferation. Hypoxia also induced the expression of liver genes needed for enhanced anaerobic ATP production of gluconeogenesis. These responses may represent an important adaptive strategy enabling *G. mirabilis* to survive under natural conditions of environmental hypoxia (15). A similar study showed that zebrafish embryos are able to survive even in the total absence of oxygen (anoxia, 0% O₂) (32). In this study, following 24 h of 0% oxygen, zebrafish embryonic development ceased and the embryos entered a state of suspended animation. Further analysis of the anoxia-exposed zebrafish embryos revealed that blastomeres were arrested during the S and G₂ phases of the cell cycle (32). However, the molecular basis of the zebrafish response to hypoxic stress has not been clarified. Understanding how hypoxia alters gene expression will likely contribute to our knowledge of how vertebrates in general respond to hypoxia and will illustrate the dynamic interactions between genes and environment.

To better understand how zebrafish respond to hypoxia at the gene level, we constructed a cDNA microarray containing 4,512 unique zebrafish genes identified from zebrafish embryonic (3-day-old) hearts, adult hearts, and skeletal muscle cDNA libraries. We then used this microarray to examine the gene expression profile of zebrafish embryos exposed to 24 h of hypoxia during development. Our findings indicate that hypoxia induces changes in gene expression in the zebrafish and that these expression patterns are recovered upon reexposure to a normoxic (20.8% O₂) environment. Our study utilizes microarray technology to reveal dynamic changes in levels of zebrafish gene expression in relation to development and survival of the zebrafish embryos in response to hypoxic stress.

MATERIALS AND METHODS

Fish stocks and hypoxia exposures. Zebrafish were obtained from a local pet store, raised, and handled according to standard methods. Adult fish were kept at 28°C on a 14-h light/dark cycle. Zebrafish embryos were staged and sorted according to Kimmel et al. (22). For hypoxic time course experiments, 48 h postfertilization (48 hpf) zebrafish embryos were exposed to 5% oxygen for the last 24 h ("HYPO") using an oxygen controller (Coy Laboratory Products). Embryos were incubated in the hypoxic chamber at 28°C for 24 h and then were quickly removed and stored in liquid nitrogen for RNA extractions. For posthypoxia experiments, 24 hpf

Article published online before print. See web site for date of publication (<http://physiolgenomics.physiology.org>).

Address for reprint requests and other correspondence: C. C. Liew, The Cardiovascular Genome Unit, Brigham and Women's Hospital, Harvard Medical School, 75 Francis St., Boston, MA 02115 (E-mail: cliew@rics.bwh.harvard.edu).

embryos were first subjected to hypoxia for 24 h then exposed to normoxic environment for an additional 5 h ("POST-HYPO"). At least 50 embryos were allowed to recover in normoxic environment and were raised to 3 days old. The remainder were collected and stored in liquid nitrogen following 5 h of exposure to a normoxic environment. At least three independent batches of embryos were collected for each experiment.

cDNA microarray constructions. Microarray slides were produced as previously described (1). A 4,512-unique element zebrafish cDNA microarray was constructed. The array consisted of PCR amplicons generated from zebrafish embryonic heart (3-day-old) (39) and adult heart and adult skeletal muscle cDNA libraries (38). To date we have generated more than 11,000 expressed sequence tags (ESTs) from these three cDNA libraries. The ESTs have been processed with the TIGR Assembler to establish a nonredundant set of ESTs. Approximately 4,500 unique ESTs have been identified, comprising 3,159 embryonic heart ESTs, 736 adult heart ESTs, and 617 skeletal muscle ESTs. A complete list of all the genes on our cDNA microarray can be viewed at our website (<http://tcgu.bwh.harvard.edu/zebrafish/Hypoxia%20Genes.htm>) and is also available as Supplementary Material at the *Physiological Genomics* web site.¹

In addition to zebrafish PCR amplicons, we included on the array 192 PCR amplicons from bacteria to serve as controls for labeling, hybridization, and fluorescent background. PCR products produced from our previously isolated and sequenced bacteriophage stock were used as the DNA substrate for the array. Approximately 30–50 µg of PCR product was produced per 50-µl reaction for each cDNA clone in a 96-well plate format. PCR products were purified using a standard ethanol precipitation procedure. Prior to spotting, the PCR products were resuspended in 25 µl of 3 × saline sodium citrate (SSC) (final concentration of 150–175 ng/µl) overnight.

PCR products were spotted onto Corning CMT GAPS microarray slides using an Affymetrix 417 X-Y-Z robotic arrayer (Santa Clara, CA) currently available in our facility. Approximately 7.5 pg of PCR product was spotted onto the array to generate each spot (~50 pl/spot of 150–175 ng/µl PCR product). Following spotting, the arrays were moistened over a hot water bath, snap dried, and the DNA was covalently cross-linked to the slide using ultraviolet irradiation. Blocking of the arrays was done by soaking each slide in a solution containing 1% (wt/vol) bovine serum albumin for 30 min at 50°C. DNA on the array was denatured by placing the array in a 95°C water bath for 3 min followed by snap cooling in an ice-cold 95% ethanol bath. Slides were then dried in a slide rack by centrifugation at 1,000 rpm for 2 min and were stored in the dark at 25°C.

For quality control, 1 slide from each batch of 42 was checked for DNA spot quality. This was done by soaking the slides in a solution of diluted SYBER Green II DNA stain (Molecular Probes). SYBER Green II is an intercalating dye that binds specifically to single-stranded DNA.

cDNA microarray experiments. We examined the following five time points: normal 24 hpf embryos, 48 hpf embryos that were exposed to 5% oxygen for the last 24 h (HYPO), 53 hpf embryos that were hypoxia treated as described then exposed to normoxia for an additional 5 h (POST-HYPO), normal untreated 29 hpf, and normal untreated 48 hpf embryos.

Each experiment was done 3 times, representing a total of 15 slides. Total RNA was extracted from control, tested embryos, and reference (12 hpf) using TRIzol reagent (GIBCO-BRL, Life Technologies). Labeling and hybridization were performed as previously described (38). Briefly, for the labeling process, 35 µg of each RNA species (i.e., 24 hpf, HYPO, POST-HYPO, 29 hpf, and 48 hpf) were oligo-dT primed and labeled in the presence of Cy5-dUTP (Amersham Pharmacia) at 42°C. A parallel labeling with Cy3-dUTP was performed with reference RNA (12 hpf). Unincorporated Cy3 and Cy5 dyes were removed from the target mixture by gel exclusion chromatography (ProbeQuant G-50, Amersham). The two targets (one Cy3 and one with Cy5) were mixed in 40 µl hybridization buffer [50% formamide, 6 × SSPE, 0.5% SDS, 5× Denhardt's solution, plus blocking agents poly-dA (2 µg), tRNA (4 µg), and calf thymus DNA (10 µg)]. The labeled target mixture was then denatured and hybridized to slides overnight at 37°C. After hybridization, the slides were washed in 2× SSC for 1 min followed by three washes of 2× SSC/0.1% SDS for 15 min each at 50°C. Slides were then rinsed in 2× SSC followed by a 1-min spin at 1,000 rpm to remove excess fluid. The slides were scanned using an Affymetrix 418 Array Scanner at 635 nm (Cy5) then at 532 nm (Cy3), and fluorescent intensities were quantified using ScanAlyze 2.44 microarray image analysis software (13) (Michael Eisen, Stanford University, CA).

cDNA microarray data processing. Local background was subtracted from the fluorescent value of each spot to obtain a net value. Spots whose net fluorescent value did not exceed the mean value obtained from the 192 bacteria control spots were excluded. To account for incomplete hybridization on each spot, we included in our analysis only those spots in which at least 50% of pixels displayed fluorescence at least 1.5 times greater than local background in all experiments. All subsequent analysis was done with the software program GeneSpring (version 3.2.2; Silicon Genetics) as previously described (27). The fluorescence units of each spot represented more than once on each slide were averaged, and the ratio was then taken of the signal (tested sample):reference. The three slides representing three different RNA pools for each experiment were grouped together and treated as replicates. To identify hypoxia-induced genes, data were normalized against control (24 hpf embryos). Variations among experiments were normalized by normalizing the ratios (tested:control) from each replicate experiment to 1.0. A Student's *t*-test was performed to calculate whether the mean relative intensity for a gene was statistically different from 1.0 (27). We used control-only comparisons (24 hpf) to determine the cutoff values for up- or downregulated genes. Three control experiments were done, and the standard deviation for more than 4,500 genes on the array from each experiment was 0.19, 0.22, and 0.21, respectively. The average standard deviation from the three experiments was 0.2. On the basis of this, we chose >1.6 as the cutoff value for upregulated genes and <0.6 for downregulated genes. We believe that 3 SD is a conservative criterion for gene selection. Genes were considered differentially expressed if they were present in at least two of three replicate experiments and were statistically significantly different ($P < 0.05$) from the controls (i.e., 24 hpf).

Verification of gene expression using quantitative real-time RT-PCR. To confirm the expression patterns of a few candidate genes, we used quantitative RT-PCR in 96-well format (Applied Biosystems, Foster City, CA) to analyze the expression of 10 transcripts: HIF-1 α , lactate dehydrogenase (LDHa), calcium ATPase, creatine kinase 3 (CKM3), cytochrome C subunit 1 (CYTO1), NADH dehydrogenase subunit 4L (NAD4L), erythropoietin (EPO), globin bA1, skeletal muscle myosin

¹The Supplementary Material for this article is available online at <http://physiolgenomics.physiology.org/cgi/content/full/13/2/97/DC1>.

light chain 3 (MYLZ3), and parvalbumin- β (PVALb). RT-PCR reactions ($n = 3$) were performed for each gene of interest. As an internal control, primers for β -actin were designed and amplified in parallel with the genes of interest. One-step RT-PCR reactions were performed using 100 ng of total RNA per reaction. Primers were designed online (http://www-genome.wi.mit.edu/cgi-bin/primer/primer3_www.cgi). The primer sequences were as follows: 1) HIF-1 α , forward 5' CCAGTGGAACCAGACATCAG 3', reverse 5' AGGAGGGTAAGGGTTGGAAT 3'; 2) LDHa, forward 5' CACAGTTGAAGATGGCCTCA 3', reverse 5' TGTGCGTCTTGAGAAACAGG 3'; 3) ATPase, forward 5' TGGTGATGGTGTCAATGATG 3', reverse 5' TAGCTCTGCCTTCCTCAACA3'; 4) CKM3, forward 5' AGGCAACTGACAAGCACAAG 3', reverse 5' ACTCTCCATC-CAGCTGCTC 3'; 5) CYTO1, forward 5' ACTTAGCCAAC-CAGGAGCAC 3', reverse 5' GGGTGGAAGAAGTCAGAAGC 3'; 6) NAD4L, forward 5' CATTTCACCGTGTTCACCTC 3', reverse 5' TTCGAGCTGTGGCTACTAGG 3'; 7) EPO, forward 5' ACCAAACAGCGTTGTGATGA 3', reverse 5' TACTTGCCTTTGGGAAATGG 3'; 8) globin bA1, forward 5' TTCTCACTGGGCTGACTTGA 3', reverse 5' TCGACTGACACGTGAACCTC 3'; 9) MYLZ3, forward 5' GTAAGAACCACCAACAAG 3', reverse 5' GGTTCGCTCATCTTCTCACC 3'; 10) PVALb, forward 5' GGAATTCTCAAGGACGAGGA 3', reverse 5' TGCAGGAACAGTTTCAGCTC 3'; and 11) β -actin, forward 5' TTCTGTTCGGTACTACTGGTATTGTG 3', reverse 5' ATCTTCATCAGGTAGTCTGTCAGGT 3'. All reactions were carried in 50- μ l volumes containing 1 \times SYBER Green PCR Master Mix, 0.25 U/ μ l Multiscribe reverse transcriptase (Perkin-Elmer), 0.4 U/ μ l RNase inhibitor, and 10 pmol of each forward and reverse primer. Reactions in 96-well format were performed in the Perkin-Elmer ABI Prism 7700 sequence detection system. The cycling parameters were 30 min at 48°C, followed by 40 cycles of 30 s at 94°C and 1 min at 60°C.

RESULTS

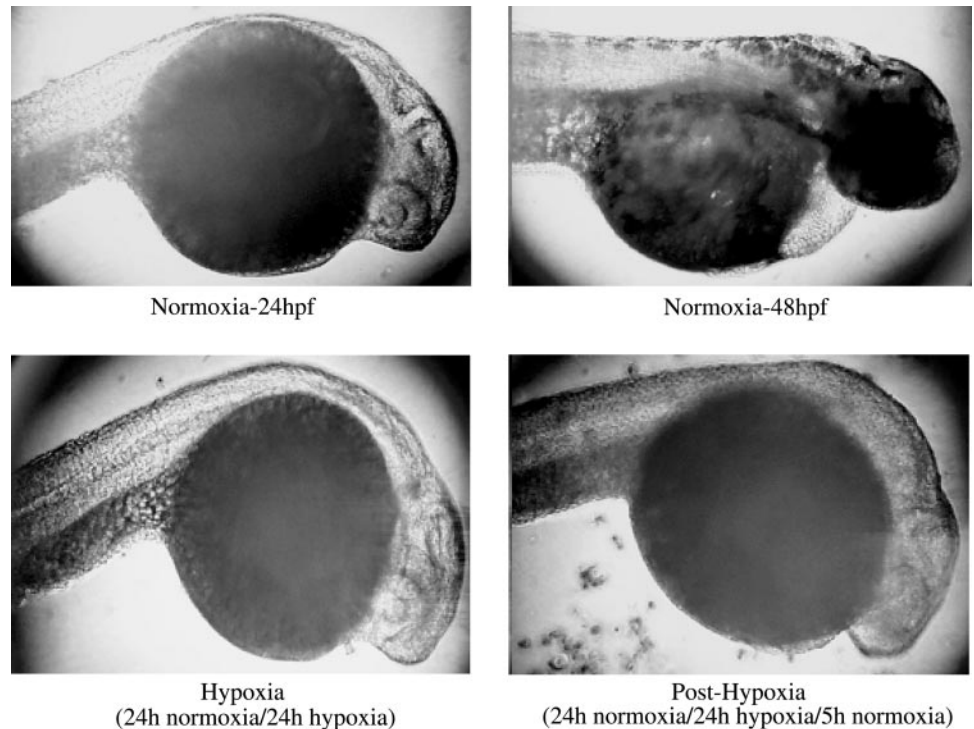
Microarray construction. Differential gene expression analyses using cDNA microarrays have been applied to model organisms such as the yeast *Saccharomyces cerevisiae* (11), *D. melanogaster* (14), the mouse (29), and the rat (35). To date, however, cDNA microarrays have not been developed for the zebrafish, and there is an urgent need for the development and application of this technology to fully exploit the zebrafish on a genomic scale. Our preliminary pilot microarrays were constructed with 1,326 unique ESTs identified from our 3-day-old zebrafish embryonic heart cDNA library (39). Our initial experiments used poly-L-lysine-coated slides from Sigma. In subsequent experiments, we spotted cDNA onto aminosilane-coated slides from Corning. Although the hybridizations from both slides were successful, the aminosilane-coated slides gave superior signals and fewer background signals. To give a better representation of clones on our microarray, we constructed two more cDNA libraries from zebrafish adult heart and skeletal muscle. To prepare the second-generation zebrafish cDNA microarray, we printed 4,512 unique cDNAs including 2,371 known genes, 624 ESTs, and 1,517 novel ESTs from 3 different cDNA libraries: embryonic heart, adult heart, and skeletal muscle; 192 bacteria PCR amplicons were also included on the array as controls for labeling, hybridization, and fluorescent background (39). It is likely that this set of 4,512 ESTs contains redundancy. One of the

disadvantages of generating sequence clusters through nucleotide sequence comparisons is that several clusters of a single gene transcript can be formed, mainly as a result of long transcripts and alternative splicing (10).

Hypoxia exposure. In this study we examined how embryonic zebrafish gene expression pattern changes under 24-h hypoxia by assaying whole embryos at the following four different time points: HYPO (48 hpf embryos were exposed to 5% oxygen for the last 24 h), POST-HYPO (53 hpf embryos that were hypoxia treated as described then exposed to normoxia for an additional 5 h), normal untreated 29 hpf, and normal untreated 48 hpf relative to 24 hpf. The ability of the zebrafish embryo to survive in an anoxic (0% O₂) environment has recently been documented; in anoxia the embryos enter a state of suspended animation and development stops (32). For the purposes of our study, it was necessary to establish a critical level of oxygen tension (P_{O₂}) low enough to induce hypoxia but sufficient to ensure the embryos' survival. We chose a P_{O₂} of 5%, a level of hypoxic stress that is tolerated by 24 hpf embryos for 24 h. We noted that tolerance to hypoxia in zebrafish is affected by developmental stage. We found that zebrafish embryos 24 hpf and younger were capable of surviving for 24 h at 5% oxygen, and we observed that during this period, embryonic development stopped (Fig. 1). To show at the gene level that hypoxia-treated embryos are developmentally arrested, we included expression data from normal 48 hpf embryos in our analysis (Fig. 2). As embryos get older, they become very sensitive to hypoxic stress. Upon reexposure to normoxic environment, the embryos continued to develop normally. As a control experiment, we monitored 50 embryos from each hypoxia experiment for an additional 3 days. These embryos developed normally, were able to swim, and were indistinguishable from fish raised under normal conditions. The ability of zebrafish embryos to survive, recover, and develop normally after exposure to hypoxia has also been documented by Padilla and Roth (32).

Microarray data analysis. For the microarray experiments, reference RNA taken from 12 hpf embryos was used as the Cy3-labeled reference sample, and RNA from other time points was labeled with Cy5. Data was normalized against control 24 hpf embryos. By 24 hpf, the body plan of the zebrafish embryo is well established and the heart and musculature structures can easily be seen under the microscope. By 48 hpf most of the internal organs are developed, including the cardiovascular system, gut, liver, and kidney. From our previous analysis of gene expression of the zebrafish during embryonic development (38), we estimate that 90–95% of genes on the array are expressed at 24 hpf. To control for variation among experiments, RNA from more than three independent batches of embryos at each time point was collected. To show that hypoxia-treated embryos are developmentally arrested both at the morphological and the gene levels, we included data from normal 48 hpf embryos in the clustering analysis. Our preliminary analysis of gene expression

Fig. 1. Zebrafish embryos arrested when exposed to 5% oxygen. Zebrafish embryos at 24 h postfertilization (24 hpf) were collected and exposed to either a normoxic environment (20.8% oxygen) or hypoxia (5% oxygen). *Top left*: 24 hpf zebrafish embryos were exposed to normoxic environment (20.8% oxygen) (Normoxia). *Top right*: 48 hpf zebrafish embryos were exposed to normoxia environment. *Bottom left*: 48 hpf zebrafish embryos were exposed to hypoxia (5% oxygen) for the last 24 h (Hypoxia). *Bottom right*: 53 hpf embryos that were hypoxia treated then exposed to normoxia for an additional 5 h (Post-Hypoxia).



in zebrafish exposed to hypoxia was done with the first-generation zebrafish microarray (1,326 ESTs from the 3-day zebrafish embryonic hearts cDNA library). For this pilot validation study, RNA from treated 60 hpf embryos (36 hpf embryos exposed to 5% oxygen for the last 24 h) was labeled with Cy5 and compared against Cy3-labeled control RNA (normal 36 hpf embryos). A total of 44 differentially expressed genes were identified. We observed changes in gene expression that correlate to known hypoxia responses in other organisms. These include the induction of glycolytic enzyme genes and the suppression of genes encoding for contractile, structural, and metabolic proteins. This validation pilot study encouraged us to test our hypothesis on a larger scale using a second-generation zebrafish microarray. A total of 33 of 44 genes (75%) were identified in this study. Genes that were not identified included different isoforms of collagens and keratins, possibly because older embryos (36 hpf) were used in the pilot experiment.

In this study we identified a total of 138 hypoxia responsive genes (Fig. 2). To analyze and interpret the data, we clustered differentially expressed genes according to their temporal expression patterns, using a hierarchical clustering program (38). Figure 2 shows the cluster image of the hypoxia-induced genes. Expanded annotated clusters with numerical data from Fig. 2 and accession numbers are listed on our web site (<http://tcgu.bwh.harvard.edu/zebrafish/Hypoxia%20Genes.htm>). Many of the genes that displayed differential expression encode proteins with known functions; others correspond to genes of unknown function, including novel genes and ESTs, suggesting that these genes may be involved in as yet

uncharacterized aspects of zebrafish adaptive responses to hypoxia. Using our previously established classification scheme, we classified genes on the basis of their biological functions (19). Many of the hypoxia-responsive genes identified are consistent with other animal model systems. These included the suppression of contractile/structural genes and the induction of hypoxia-inducible factor 1 α (HIF-1 α) and components of the glycolytic pathway such as aldolase, enolase, and phosphoglycerate mutase (Fig. 3). A limitation of our analysis is a lack of internal standards. We did not spike the target with various dilutions of labeled bacterial target to determine the sensitivity of the array.

Quantitative real-time RT-PCR analysis. We used real-time RT-PCR to confirm the changes in mRNA levels that were identified for a few selected genes during exposure to hypoxia. Primers were designed for HIF-1 α , lactate dehydrogenase, calcium ATPase, creatine kinase 3, cytochrome C subunit 1, NADA dehydrogenase subunit 4L, erythropoietin, globin bA1, skeletal muscle myosin light chain 3, and parvalbumin- β . Figure 4 shows that changes in mRNA levels are consistent with the microarray data. However, microarray data tended to underrepresent the change relative to real-time RT-PCR. Changes of 2-fold (skeletal myosin light chain 3) to 2.5-fold (parvalbumin- β) during post-hypoxia were detected with real-time RT-PCR, whereas changes detected by microarray hybridization were \sim 1.5 to 2-fold for myosin light chain 3 and parvalbumin- β , respectively.

DISCUSSION

Zebrafish embryos can survive for 24 h in the absence of oxygen (anoxia, 0% O₂). Padilla and Roth (32)



Fig. 2. Cluster images of 138 hypoxia-induced genes expression profile. HYPO, 48 hpf embryos were exposed to 5% oxygen for the last 24 h; POST-HYPO, 53 hpf embryos that were hypoxia treated then exposed to normoxia for an additional 5 h. Gene expression is shown in rows. The quantitative changes in genes expression are represented in color: red indicates that a gene is more highly expressed at the time point than controls, and green indicates repressed genes. Expanded annotated figures showing the gene names and expressed sequence tags (EST) accession numbers are posted on our web site (<http://tcgu.bwh.harvard.edu/zebrafish/Hypoxia%20Genes.htm>) and are also available from the *Physiological Genomics* web site.

showed that in such an anoxic environment, zebrafish enter a state of suspended animation in which cell division stops and developmental progression ceases. In this study we assayed whole zebrafish embryos at four different time points (HYPO, POST-HYPO, 29 hpf, and 48 hpf) to examine how embryonic zebrafish gene expression patterns change when exposed to 24 h of hypoxia. Our study illustrates the gene-level adaptive mechanisms of zebrafish embryonic survival by showing 1) that hypoxia triggers changes in gene expression and 2) that these changes are reversed upon reexposure to normoxia.

A measure of the reliability of our experiments was that we showed the induction of HIF-1 α . Hypoxia-triggered HIF-1 α increases are known to upregulate the expression of a number of genes involved in alternative metabolic pathways that do not require oxygen (glycolysis) (36). HIF-1 α also plays a role in development and is regarded as a master regulator of cellular and developmental oxygen homeostasis (21).

In the face of falling oxygen supplies, fish respond first by reducing energy metabolism and later by increasing energy supplies from anaerobic sources (21, 42, 43, 50). In humans and other air-breathing vertebrates, hypoxia leads to rapid adaptive changes such as the activation of anaerobic ATP-generating pathways, such as glycolysis. Zebrafish undergo a metabolic switch when exposed to hypoxia: tricarboxylic acid (TCA) cycle enzymes such as succinate dehydrogenase, malate dehydrogenase, and citrate synthase are repressed, whereas a number of glycolysis pathway genes are upregulated, including phosphoglycerate mutase, kinase, aldolase, and enolase (Fig. 3A). The coordinated repression of TCA cycle enzymes and upregulation of glycolysis pathway components indicates a shift from aerobic oxidation to anaerobic glycolysis under hypoxia. Further evidence for hypoxia-induced glycolysis is the induction of lactate dehydrogenase. With low levels of available oxygen to support aerobic oxidation of the pyruvate produced from glycolysis, pyruvate can be reduced to lactate by the enzyme lactate dehydrogenase. Hypoxic tissues in mammals show increased intracellular levels of adenosine, resulting from metabolism of *S*-adenosylhomocystein to adenosine. The expression of adenosine homocysteine hydrolase increases in zebrafish embryos during hypoxia (Fig. 3A). This enzyme is important in mediating the conversion of *S*-adenosylhomocystein to adenosine and homocysteine. Adenosine action includes reducing energy demands and at the same time increasing oxygen supply by vasodilatation of vessels locally (reviewed by Poulsen and Quinn, Ref. 33). It has also been reported that adenosine plays a similar protective role in fish (3, 4). Our findings that HIF-1 α and other genes of the glycolytic pathway are induced under hypoxia are consistent with work in other animal model systems (15, 32).

One of the most important defense mechanisms against hypoxia in animals is the downregulation of energy consumption (17). In our study we showed that hypoxia triggered a strong coordinated downregulation

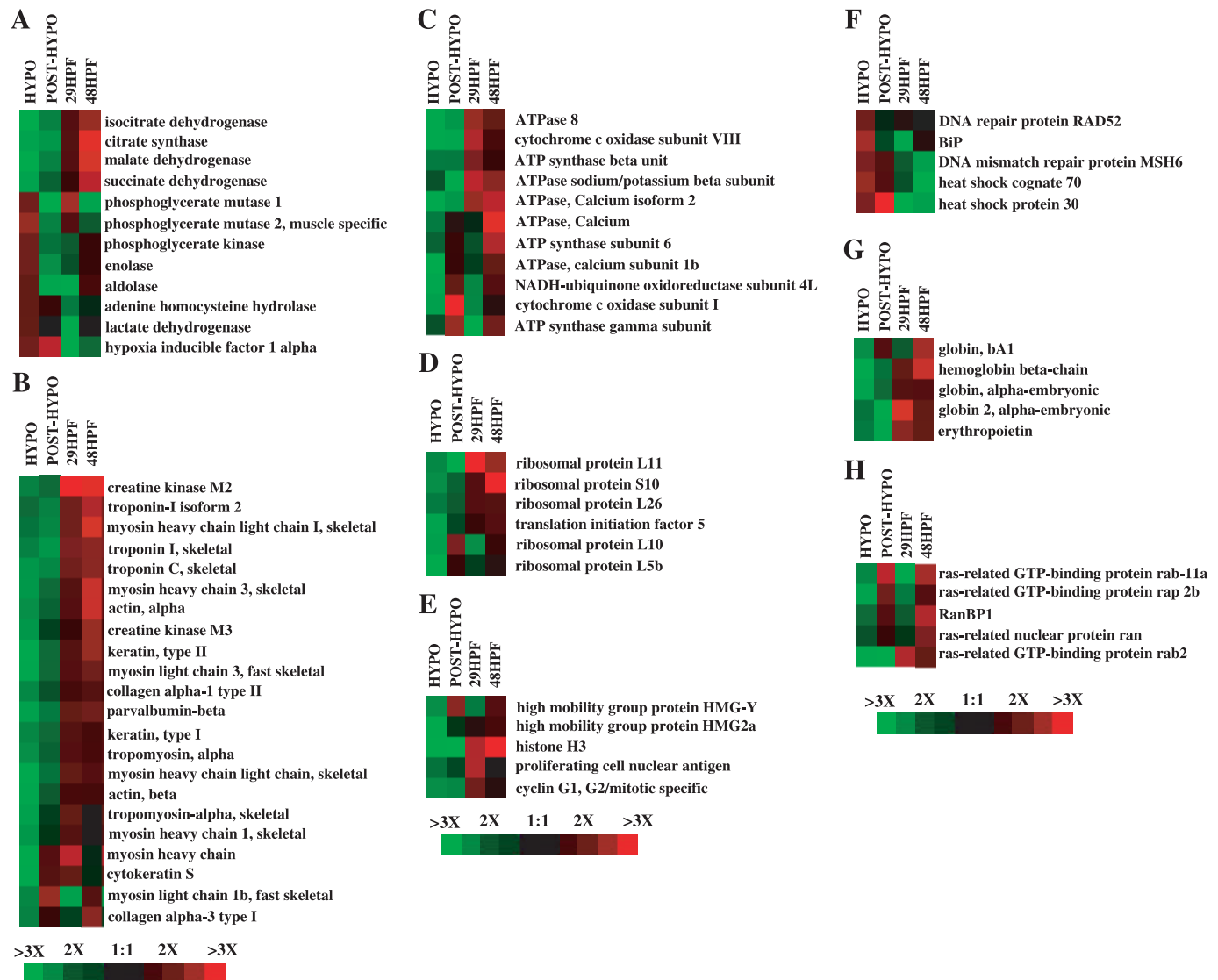


Fig. 3. Selected genes from data presented in Fig. 2 and grouped into categories on the basis of their biological roles: glycolysis/TCA (A), cell structure/motility (B), metabolism (C), protein expression (D), cell division (E), cell/organism defense (F), globins synthesis (G), cell signaling/communication (H). Time points in hours are indicated above each column. Gene expression is shown in rows. The quantitative changes in genes expression are represented in color: red indicates induced genes, and green indicates repressed genes.

of genes encoding for contractile, extracellular matrix, and cytoskeletal proteins (Fig. 3B). Since cell structure and motility proteins are highly abundant proteins, reducing their expression during hypoxia may represent an important energy-saving strategy. Strong downregulation of other proteins involved in muscle contraction, such as parvalbumin, was also detected. Parvalbumin is a muscle calcium binding protein that plays an important role in the contraction-relaxation cycle of fish skeletal muscles (40). Consistent with the decrease in muscle contraction and metabolism, muscle creatine kinase mRNA levels decline during hypoxia (Fig. 3B), suggesting that the demand for phosphocreatine falls (15).

Other mechanisms to reduce energy costs include the suppression of ion channel densities and/or channel leak activities to lower the energy costs of ion-balan-

ing ATPases (6). Suppression in expression of channel ATPases was detected during hypoxia (Fig. 3C). This “channel arrest” phenomenon has also been reported in a hypoxia-tolerant turtle (24). Hypoxia-induced reduction in membrane permeability helps to ensure cell survival by maintaining cell membrane potential and, in particular, by controlling ion influxes between cellular compartments and the external environment (25).

We also observed a strong repression of genes encoding for elements of the protein translation machinery, such as ribosomal proteins and translation initiation (Fig. 3D). A similar observation was made in *G. mirabilis* in hypoxic conditions (15). Protein synthesis is energy costly; it is the only energy-requiring process that is more costly than ion-pumping ATPase activity (25). Thus turning protein synthesis rates down to

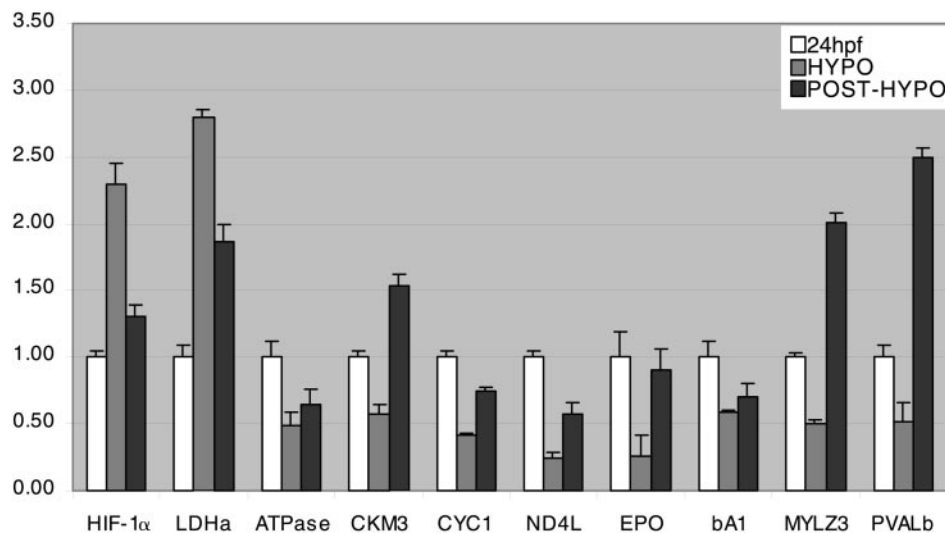


Fig. 4. Real-time RT-PCR results of a number of selected genes identified by the microarray analysis. Abundance of mRNA levels was compared against 24 hpf for hypoxia-inducible factor α (HIF-1 α), lactate dehydrogenase (LDHa), calcium ATPase (ATPase), creatine kinase 3 (CKM3), cytochrome C subunit 1 (CYC1), NADH dehydrogenase subunit 4L (ND4L), erythropoietin (EPO), globin bA1 (bA1), skeletal muscle myosin light chain 3 (MYLZ3), and parvalbumin- β (PVALb).

minimal levels may represent an important adaptive strategy for survival under hypoxia. In principle, hypoxia-induced repression of protein synthesis could occur at the level of gene transcription or translation (17). Although we do not clearly understand the mechanisms of hypoxia-induced repression of protein synthesis in animal models, hypoxia-induced suppression of protein synthesis in plants is known to be mediated by a translational block affecting both initiation and elongation (17). It has been shown that hypoxia-induced translational arrest results from the failure of elongation factor 1 α (EF-1 α) to dissociate from ribosomes during the elongation cycle (44). Other genes encoding for proteins involved in energy metabolism, such as components of the electron transport chain, were also downregulated during hypoxia. The suppression of ion pumping activity and the decline in protein synthesis should account for the bulk of energy savings and may be necessary for a long-term hypoxia survival strategy.

Of interest, we observed the repression of several genes involved in cell division such as cyclin G1 and proliferating cell nuclear antigen (Fig. 3E). This is consistent with earlier observations that hypoxic zebrafish embryos are developmentally arrested and that in anoxia zebrafish cells arrest in the S and G₂ phases of the cell cycle (32). We also detected the induction of a number of genes involved in cellular defense (Fig. 3F). For example, we observed elevated expressions of chaperone proteins such as heat shock proteins 70 and 30. It is known that heat shock proteins are rapidly induced by such stresses as mechanical stretch, hypothermia, and hypoxia (47). Previous studies have demonstrated ischemia-induced heat shock protein 70 (HSP70) gene expression in tissues of intact animals (12) and in cultured cells (2). HSP70 functions as a chaperone and is also known to protect cells against apoptosis (18). A strong induction of the stress-inducible immunoglobulin binding protein, BiP, was also

observed. BiP is an important component of the endoplasmic reticulum stress response of cells and is involved in protein translocation, folding, and degradation (16). Its expression is markedly induced in ischemic neurons (20), and its functions are essential to cell viability (16). In addition, two genes encoding for DNA repair, RAD52 and DNA mismatch repair MSH6, were also induced. Acute hypoxia has been shown to induce DNA strand breaks (35) and an increase in the number of DNA strand breaks has also been reported in fish under hypoxic conditions (26). Thus the expression of these genes may serve a protective role against cell ischemic injury under exposure to hypoxia.

Unexpectedly, hypoxia did not result in upregulation of genes encoding for erythropoietin and globins (Fig. 3G). Hemoglobin-oxygen affinity is known to increase in fish during hypoxia in order that hemoglobin saturation can be maintained under conditions of falling blood oxygen levels (41). Red blood cell production can also be increased during hypoxia in mammals and is stimulated by the hormone, erythropoietin (23, 45). A possible explanation for the lack of hypoxia-induced erythropoietin and globin upregulation this study is that zebrafish embryos at 24 hpf do not require blood flow for survival: oxygen uptake can be achieved through diffusion (46). In addition, suppression of protein synthesis represents the greatest protection against, and hence advantage for survival in, hypoxia.

We detected the suppression of a number of intracellular transducers such as small GTP-binding proteins during hypoxia (Fig. 3H). Rab proteins exist in all eukaryotic cells, and they are known to regulate intracellular vesicle trafficking (9). Ran is another member of the small GTP protein family known to regulate nucleocytoplasmic transport and microtubule organization during cell cycle (7). Ran is cyclically activated and inactivated by the GTP-Ran binding protein 1 (RanBP1) (5). These small G proteins are required for various cell functions such as establishment of cell

polarity, cytokinesis, and cell motility (for review, see Takai et al., Ref. 37). The downregulation of these proteins during hypoxia indicates the repression of cell signaling/communication, and their coordinated downregulation may be related to the suppression of cell growth and proliferation under hypoxia.

The ability of zebrafish to recover from anoxia has been reported (32); however, the molecular mechanisms of how zebrafish respond to and recover from hypoxia are unclear. Our expression profile reveals that hypoxia induces changes in gene expression and that these patterns revert to normal upon reexposure to normoxia. For example, HIF-1 α and enzymes of the glycolytic pathway are upregulated during hypoxia: their expression declines at normal oxygen levels (Fig. 3A). Similarly, many genes encoding for contractile, cytoskeletal, and ribosomal proteins decreased expression under hypoxia but partially recovered upon reexposure to normoxia (Fig. 3, B and D). Compared with the normal 29 hpf embryos, the expression patterns of the posthypoxic embryos are lower because these zebrafish embryos are still in a recovery phase. Padilla and Roth (32) reported that when zebrafish embryos were exposed to anoxia for more than 19 h, ~6 h of exposure to air was required for the animals' heart rates to return to normal. Anoxia induced suppression of protein synthesis, and recovery has also been observed in hypoxia-tolerant turtles (25).

Real-time RT-PCR is a useful method for validating microarray data. Overall, real-time RT-PCR confirmed the regulation of the 10 selected genes. However, differences were seen in the magnitude of expression differences between microarray and real-time PCR data. Microarrays tend to have a low dynamic range, which can lead to underrepresentations of fold changes in gene expression (8, 31, 34). This might arise either from overestimating the noninduced genes due to non-specific hybridization or from underestimating the level of induction due to target saturation effects (49). As RT-PCR has a greater dynamic range, it is often used to validate the observed trends rather than duplicate the fold changes obtained by microarray experiments (28, 48).

Our study provides a global view of gene expression patterns in the zebrafish embryo in response to hypoxic stress. In addition, by identifying zebrafish genes and groups of genes known to function together in pathways induced by hypoxia, we are able to demonstrate the power of microarray technology to study gene expression on a global scale. The coordinated changes in gene expression that we observed are consistent with findings in other model systems. The data presented in this study help to clarify some of the adaptive mechanisms by which the zebrafish responds to and recovers from hypoxia. Our data show that under hypoxia, zebrafish embryos undergo wide-scale changes in gene expression, including a series of hypoxia-defense processes. One such defense is a drastic suppression of ATP demand, including shutting down costly energy processes such as protein synthesis, cell division, and

ion pumping activity. Another physiological hypoxia-defense strategy involves reorganizing metabolic pathways by switching from aerobic oxidation to the glycolytic pathway. A further defense occurs concurrently, as cellular stress responses are induced which may serve a protective role against ischemic injury during hypoxia. Upon reexposure to normoxia, these hypoxia-induced gene expression patterns are reversed.

We believe that we have clearly shown how gene expression patterns in the zebrafish change in response to hypoxia. However, it is difficult to determine which changes are the direct effects of hypoxia and which may be the indirect effects of developmental arrest. Further studies are needed to identify the molecular pathways that are responsive specifically to hypoxia. For example, antisense morpholinos can be used to target HIF-1 α or other genes known to be activated by HIF-1 α such as erythropoietin, and the enzymes of glycolysis before hypoxic treatment. It must be emphasized that this study does not attempt to fully identify specific genes and pathways that respond to hypoxia. Our intention is rather to provide a preliminary view of global changes in gene expression in zebrafish embryos under hypoxia and to highlight the effectiveness and potential of microarray technology for zebrafish studies. Despite the limited number of genes on our array, we observed global changes in gene expression that correlate to hypoxia defense mechanisms of the zebrafish embryos. With the completion of the zebrafish genome-sequencing project, a more comprehensive genome-wide analysis of gene expression will be possible. Such studies will be invaluable for analyzing the hundreds of mutants that affect zebrafish embryonic development.

We thank Victor Dzau for his support, and we thank Richard Pratt, Leonard Anderson, David Barrans, and John Chen for helpful comments and suggestions. We thank Isolde Prince and David Kaicher for editing this manuscript. We especially thank Richard Lee and Gilles Dekeulenaer for help with the hypoxic chamber.

This work was supported in part by grants from the Heart and Stroke Foundation of Canada and the Canadian Institute of Health Research. C. Ton is a recipient of a Heart and Stroke Foundation of Canada Scholarship.

REFERENCES

1. **Barrans JD, Stamatiou D, and Liew CC.** Construction of human cardiovascular cDNA microarray: portrait of the failing heart. *Biochem Biophys Res Commun* 280: 964–969, 2001.
2. **Benjamin IJ, Kroger B, and Williams S.** Activation of the heat shock transcription factor by hypoxia in mammalian cells. *Proc Natl Acad Sci USA* 87: 6263–6267, 1990.
3. **Bernier N, Harris J, Lessard J, and Randall D.** Adenosine receptor blockade and hypoxia-tolerance in rainbow trout and Pacific hagfish. I. Effects on anaerobic metabolism. *J Exp Biol* 199: 485–495, 1996.
4. **Bernier N, Fuentes J, and Randall D.** Adenosine receptor blockade and hypoxia-tolerance in rainbow trout and Pacific hagfish. II. Effects on plasma catecholamines and erythrocytes. *J Exp Biol* 199: 497–507, 1996.
5. **Bischoff FR, Krebber H, Smirnova E, Dong W, and Pongstingl H.** Co-activation of RanGTPase and inhibition of GTP dissociation by Ran-GTP binding protein RanBP1. *EMBO J* 14: 705–715, 1995.

6. **Boutillier RG and St-Pierre J.** Surviving hypoxia without really dying. *Comp Biochem Physiol A Mol Integr Physiol* 126: 481–490, 2000.
7. **Carazo-Salas RE, Gruss OJ, Mattaj IW, and Karsenti E.** Ran-GTP coordinates regulation of microtubule nucleation and dynamics during mitotic-spindle assembly. *Nat Cell Biol* 3: 228–234, 2001.
8. **Chang BD, Watanabe K, Broude EV, Fang J, Poole JC, Kalinichenko TV, and Roninson IB.** Effects of p21^{Waf1/Cip1/Sdi1} on cellular gene expression: Implications for carcinogenesis, senescence, and age-related diseases. *Proc Natl Acad Sci USA* 97: 4291–4296, 2000.
9. **Chavrier P and Goud B.** Role of ARF and Rab GTPases in membrane transport. *Curr Opin Cell Biol* 11: 466–475, 1999.
10. **Dempsey AA, Dzau VJ, and Liew CC.** Cardiovascular genomics: estimating the total number of genes expressed in the human cardiovascular system. *J Mol Cell Cardiol* 33: 1879–1886, 2001.
11. **Derisi JL, Iyer VR, and Brown PO.** Exploring the metabolic and genetic control of gene expression on a genomic scale. *Science* 278: 680–686, 1997.
12. **Dillmann WH, Mehta HB, Barrieux A, Guth BD, Neeley WE, and Ross J Jr.** Ischemia of the dog heart induces the appearance of a cardiac mRNA coding for a protein with migration characteristics similar to heat-shock/stress protein 71. *Circ Res* 59: 110–114, 1986.
13. **Eisen MB, Spellman PT, Brown PO, and Botstein D.** Cluster analysis and display of genome-wide expression patterns. *Proc Natl Acad Sci USA* 95: 14863–14868, 1998.
14. **Furlong EE, Andersen EC, Null B, White KP, and Scott M.** Patterns of gene expression during *Drosophila* mesoderm development. *Science* 293:1629–1633, 2001.
15. **Gracey AY, Troll JV, and Somero GN.** Hypoxia-induced gene expression profiling in the euryoxic fish *Gillichthys mirabilis*. *Proc Natl Acad Sci USA* 98: 1993–1998, 2001.
16. **Haas IG.** BiP (GRP78), an essential hsp70 resident protein in the endoplasmic reticulum. *Experientia* 50: 1012–1020, 1994.
17. **Hochachka PW and Lutz PL.** Mechanism, origin, and evolution of anoxia tolerance in animals. *Comp Biochem Physiol B Biochem Mol Biol* 130: 435–459, 2001.
18. **Hohfeld J.** Regulation of the heat shock conjugate Hsc70 in the mammalian cell: the characterization of the anti-apoptotic protein BAG-1 provides novel insights. *Biol Chem* 3: 269–274, 1998.
19. **Hwang DM, Dempsey AA, Wang RX, Rezvani M, Barrans JD, Dai KS, Wang HY, Ma H, Cukerman E, Liu YQ, Gu JR, Zhang J, Tsui SKW, Waye MMY, Fung KP, Lee CY, and Liew CC.** A genome-based resource for molecular cardiovascular medicine: towards a compendium of cardiovascular genes. *Circulation* 96: 4146–4203, 1997.
20. **Ito D, Tanaka K, Suzuki S, Dembo T, Kosakai A, and Fukuuchi Y.** Up-regulation of the Ire1-mediated signaling molecule, Bip, in ischemic rat brain. *Neuroreport* 21: 4023–4028, 2001.
21. **Iyer NV, Kotch LE, Agani F, Leung SW, Laughner E, Wenger RH, Gassmann M, Gearhart JD, Lawler AM, Yu AY, and Semenza GL.** Cellular and developmental control of O₂ homeostasis by hypoxia-inducible factor 1 α . *Genes Dev* 12: 149–162, 1998.
22. **Kimmel CB, Ballard WW, Kimmel SR, Ullmann B, and Schilling TF.** Stages of embryonic development of the zebrafish. *Dev Dyn* 203: 253–310, 1995.
23. **Krantz SB.** Erythropoietin. *Blood* 77: 419–434, 1991.
24. **Land SC, Sanger RH, and Smith JS.** O₂ availability modulates transmembrane Ca²⁺ flux via second-messenger pathways in anoxia-tolerant hepatocytes. *J Appl Physiol* 82: 776–783, 1997.
25. **Land SC, Buck LT, and Hochachka PW.** Response of protein synthesis to anoxia and recovery in anoxia-tolerant hepatocytes. *Am J Physiol Regul Integr Comp Physiol* 265: R41–R48, 1993.
26. **Liepert A, Karbe L, and Westendorf J.** Induction of DNA strand breaks in rainbow trout (*Oncorhynchus mykiss* Walbaum) under hypoxic and hyperoxic conditions. *Aquat Toxicol (Amst)* 33: 177–181, 1995.
27. **Manos EJ and Jones DA.** Assessment of tumor necrosis factor receptor and fas signaling pathways by transcriptional profiling. *Cancer Res* 61: 433–438, 2001.
28. **Mayanil CSK, George D, Freilich L, Mijan EJ, Mani-Farnell B, McLone DG, and Bremer EG.** Microarray analysis detects novel Pax3 downstream target genes. *J Biol Chem* 276: 49299–49309, 2001.
29. **Miki R, Kadota K, Bono H, Mizuno Y, Tomaru Y, Carninci P, Itoh M, Shibata K, Kawai J, Konno H, Watanabe S, Sato K, Tokusumi Y, Kikuchi N, Ishii Y, Hamaguchi Y, Nishizuka I, Goto H, Nitanda H, Satomi S, Yoshiki A, Kusakabe M, DeRisi JL, Eisen MB, Iyer VR, Brown PO, Muramatsu M, Shimada H, Okazaki Y, and Hayashizaki Y.** Delineating developmental and metabolic pathways in vivo by expression profiling using RIKEN set of 18,816 full-length enriched mouse cDNA arrays. *Proc Natl Acad Sci USA* 98: 2199–2204, 2001.
30. **Moller P, Loft S, Lundby C, and Olsen NV.** Acute hypoxia and hypoxic exercise induce DNA strand breaks and oxidative DNA damage in humans. *FASEB J* 15: 1181–1186, 2001.
31. **Mutch DM, Berger A, Mansourian R, Rytz A, and Roberts MA.** The limit fold change model: a practical approach for selecting differentially expressed genes from microarray data. *BMC Bioinformatics* 3: 1–11, 2002.
32. **Padilla PA and Roth MB.** Oxygen deprivation causes suspended animation in the zebrafish embryo. *Proc Natl Acad Sci USA* 98: 7331–7335, 2001.
33. **Poulsen SA and Quinn RJ.** Adenosine receptors: new opportunities for future drugs. *Bioorg Med Chem* 6: 619–641, 1998.
34. **Rajeevan MS, Ranamukhaarachchi DG, Vernon SD, and Unger ER.** Use of real-time quantitative PCR to validate the results of cDNA array and differential display PCR technologies. *Methods* 25: 443–451, 2001.
35. **Sehl PD, Tai JT, Hillan KJ, Brown LA, Goddard A, Yang R, Jin H, and Lowe DG.** Application of cDNA microarrays in determining molecular phenotype in cardiac growth, development, and response to injury. *Circulation* 101: 1990–1999, 2000.
36. **Semenza GL.** Regulation of mammalian O₂ homeostasis by hypoxia-inducible factor 1. *Annu Rev Cell Dev Biol* 15: 551–578, 1999.
37. **Takai Y, Sasaki T, and Matozaki T.** Small GTP-binding proteins. *Physiol Rev* 81: 153–185, 2001.
38. **Ton C, Stamatou D, Dzau V, and Liew C.** Construction of a zebrafish cDNA microarray: gene expression profiling of the zebrafish during development. *Biochem Biophys Res Commun* 296: 1134–1142, 2002.
39. **Ton C, Hwang DM, Demsey AA, Tang H, Yoon J, Lim M, Mably JD, Fishman MC, and Liew CC.** Identification, characterization, and mapping of expressed sequence tags from an embryonic zebrafish heart cDNA library. *Genome Res* 10: 1915–1927, 2000.
40. **Ushio H and Watabe S.** Carp parvalbumin binds to and directly interact with the sarcoplasmic reticulum for Ca²⁺ translocation. *Biochem Biophys Res Commun* 199: 56–62, 1994.
41. **Val AL.** Oxygen transfer in fish: morphological and molecular adjustments. *Braz J Med Biol Res* 28: 1119–1127, 1995.
42. **Val A, Lessard J, and Randall D.** Effects of hypoxia on rainbow trout (*Oncorhynchus mykiss*): intraerythrocytic phosphates. *J Exp Biol* 198: 305–310, 1995.
43. **van Raaij MT, Pit DS, Balm PH, Steffens AB, and van den Thillart GE.** Behavioral strategy and the physiological stress response in rainbow trout exposed to severe hypoxia. *Horm Behav* 30: 85–92, 1996.
44. **Vayda ME, Shewmaker CK, and Morelli JK.** Transnational arrest in hypoxic potato tubers is correlated with the aberrant association of elongation factor EF-1 α with polysomes. *Plant Mol Biol* 28: 751–757, 1995.
45. **Wang GL and Semenza GL.** Molecular basis of hypoxia-induced erythropoietin expression. *Curr Opin Hematol* 3: 156–162, 1996.

46. **Warren KS and Fishman MC.** "Physiological genomics": mutants screens in zebrafish. *Am J Physiol Heart Circ Physiol* 275: H1–H7, 1998.
47. **Williams RS and Benjamin IJ.** Protective responses in the ischemic myocardium. *J Clin Invest* 106: 813–818, 2000.
48. **Wurbach E, Yuen T, Ebersole BJ, and Sealfon SC.** Gonadotropin-releasing hormone receptor-coupled gene network organization. *J Biol Chem* 276: 47195–47201.
49. **Yuen T, Wurbach E, Pfeffer RL, Ebersole BJ, and Sealfon SC.** Accuracy and calibration of commercial oligonucleotide and custom cDNA microarrays. *Nucleic Acids Res* 30: 1–9, 2002.
50. **Zhou BS, Wu RS, Randall DJ, and Lam PK.** Bioenergetics and RNA/DNA ratios in the common carp (*Cyprinus carpio*) under hypoxia. *J Comp Physiol [B]* 171: 49–57, 2001.

